Ethylene Dichloride cracking reactor modelling

Susana Broeiro Bento

Chemical Engineering Department, Instituto Superior Técnico, Lisbon, Portugal
Process Systems Enterprise, London, United Kingdom

ARTICLE INFO

Date:

November 2017

Key words:

Modelling
VCM
Cracking
Radical mechanism
State estimation
gPROMS

ABSTRACT

Vinyl Chloride monomer (VCM) is one of the most important commodity chemicals and it is produced mainly by the cracking of ethylene dichloride (EDC). By-products formation is inevitable, creating several inefficiencies, and accurate model of the process is essential for its optimization

In the present work, an EDC cracker model was set-up using the furnace model from gPROMS ProcessBuilder, developed by PSE. The cracking kinetic mechanism implemented consists of 108 reversible reactions and 47 components, as reported by Choi et al. [1]

The model predictions are compared to predictions from another model which used a cracking kinetic model tuned to plant data. The deviations for the main components were in the range of 1.4-1.9%. The deviations for impurities were more significant.

A dynamic simulation of a cycle was carried out. The predictions of pressure drop, VCM flow rate and EDC flow rate over the cycle were compared to plant data. Subsequently, state estimations were performed to assess the feasibility of improving the model predictions and the initial results are positive.

Finally, a study regarding the possibility of reducing the cracking kinetic scheme was initiated. Allowing a deviation of 0.1% from the original results, it was verified that 48 reactions could be excluded without compromising the model accuracy. More tests considering other impurities in the furnace feed should be done to further validate this possible kinetic scheme reduction.

1.Introduction

The commercial significance of the vinyl chloride monomer (VCM) can be highlighted by the production of polyvinyl chloride (PVC), the world's second most abundant plastic. PVC is used in the most diverse sectors, ranging from healthcare to construction and electronics. [2]

Currently, vinyl chloride is mainly produced through the thermal cracking of ethylene dichloride (EDC). This is a balanced process, which means that all intermediates and by-products are recycled in a way that ensures a tight closure of the material balance to only VCM as the final product, starting from ethylene, chlorine and oxygen. [3] The process begins with chlorination of ethylene to ethylene dichloride:

$$C_2H_4 + Cl_2 \rightarrow C_2H_4Cl_2 \quad (1)$$

Followed by EDC dehydrochlorination to VCM, through thermal cracking according to equation 2.

$$C_2H_4Cl_2 \rightarrow C_2H_4Cl + HCl \quad (2)$$

The HCl produced during the EDC cracking is recycled to the oxychlorination section, where it is used together with ethylene to produce EDC (eq.3)

$$C_2H_4 + 2HCl + \frac{1}{2}O_2 \rightarrow C_2H_4Cl_2 + H_2O \quad (3)$$

The overall reaction (eq.4) is exothermal so the VCM plant should be able to cover a large part of its energy needs.

$$C_2H_4 + 0.5Cl_2 + 0.25O_2 \rightarrow C_2H_3Cl + 0.5H_2O \quad (4)$$

The EDC cracking takes place in a pyrolysis furnace (figure 1)

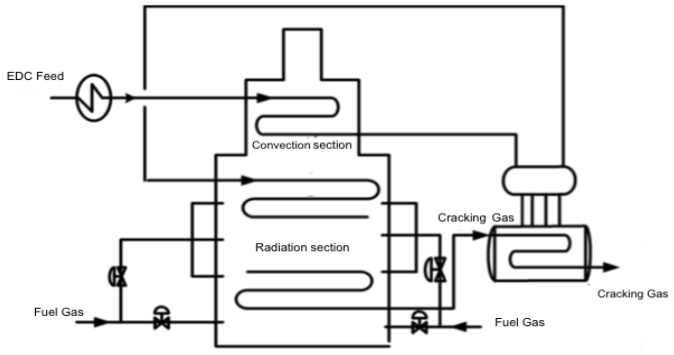

Figure 1 - EDC cracker furnace diagram

In principle, the complex thermal cracking of EDC is considered to proceed via free-radical reactions. Rigorous reaction mechanisms have been studied and

improved several times by various researchers. [4] Ranzi et al. introduced a reaction kinetic scheme with more than 200 elementary reactions with more than 40 molecular and radical species. Borsa et al. [3] developed the most complex cracking kinetic mechanism for EDC pyrolysis, including 135 compounds and radical species and more than 800 reactions. Choi et al. [1] established a mechanism that involves 108 reversible reactions and 47 molecular/radical species. The addition of carbon tetrachloride as promoter was first investigated by Choi et al. [1] Schirmeister et al. [5] simplified the EDC pyrolysis mechanism aiming the data accuracy and expenditure optimization for model adjustment. A total of 31 reactions, 18 compounds, and 8 radical species were used to describe all relevant products, intermediates, and byproducts. [4] A typical EDC conversion would be between 50 and 60%, in order to limit by-product formation and obtain selectivities to VCM around 99%. [5]

Even though it is possible to achieve high yields, the formation of by-products is inevitable, causing significant inefficiencies in the process.

Coke formation is an important reason for concern, since its deposition inside the reactor coils demands periodical shut downs of the unit. Besides coke, there are other gas phase impurities such as chloroprene and butadiene that cause down-stream difficulties in distillation columns.

Having this in consideration, it is important to accurately model the process aiming the model based process optimization.

2. Materials and Methods

In this work, the models were created and simulated in gPROMS ProcessBuilder software, developed by Process Systems Enterprise. The gPROMS advanced process modelling platform is a powerful equation-oriented modelling and optimization tool on which all of PSE's gPROMS products are built.

Besides the integral parts of gPROMS, it is also possible to use external software components, which provide a range of computational services to the models. These are defined as parameters named Foreign Object (FO) and include physical properties packages, external unit operation modules, or even complete computational fluid dynamics (CFD) software packages.

2.1 Multiflash

Multiflash is the standard gPROMS® physical properties package, supplied by KBC Advanced Technologies. It is a highly rigorous properties package, which supports all commonly-used thermo-dynamic and transport properties, including a wide range of equations of state and activity coefficient thermo-dynamic models. This is achieved with a Multiflash input file (.mfl), in which all the components, physical properties models, among other things that are necessary to the problem, are defined.

2.3 ReadData Foreign Object

With the ReadData FO, it is possible to add information to the model, regarding physical properties or even data to be use as input to the model variables. This information is obtained from a .txt file, from which is converted into arrays.

2.4 State Estimation

State estimation is a widespread and well-established technique in control engineering and weather forecasting.

If on-line data of some output variables are available, a state estimator can adjust the model prediction using these measurements to obtain a better estimate of the state. This is the most important application of on-line state estimation according to Simon. [7]

In gProms the Extended Kalman Filter is adopted, since it is one of the simplest and most important tools for state estimation purposes. [7] During state estimation, the model receives on-line measured data regarding the input and output variables. For each time unit, the estimator updates the output variable according to a prediction/correction approach. Firstly, there is the prediction step, where model equations are taken into account, followed by the correction step, where available measurements are used to correct the predicted state estimate. Hence for each instant the model will give two values for the output, resulting from each of these steps.

For each output variable and parameter a variance is defined. The variance set to the parameters can be interpreted as a measure of how much its initial value can change during state estimation, in order to meet the objective. A higher variance will allow larger change to the parameter value in comparison to a smaller variance. On the other hand, the variance of the plant data can be seen as a measure of the confidence the model can have on it. A smaller variance indicates more accuracy of the measurement and state estimation would give more importance to such measurements in comparison to those with higher variance.

To implement this technique in gPROMS, two files are required. The first is a configuration file, where all the parameters, inputs and output variables to be considered are specified, as well as their variances. The second file is a text file that contains all the plant data regarding the input and output variables.

3. Model Set-up – Furnace model

The EDC cracker was set-up using the furnace model libraries within gPROMS ProcessBuilder.

The furnace comprises several models inside of itself, consisting in three mains sections (Figure 2):

- Convection Section – Where the hydrocarbon stream is heated;

- Radiant Section (Coil) – Where cracking reactions occur;
- Transfer Line Exchanger (TLE) – Where the coil outlet stream is quickly quenched to prevent degradation of the highly reactive product through secondary reactions;

The radiant section consists of multiple coils operating in parallel. In the furnace model, each coil is assumed to behave the same and one representative coil is modelled.

Both the convection section and the coil models consist basically in several cracking tube models.

The cracking mechanism implemented was the one reported by Choi et al. [1] , consisting of 108 reversible reactions, with 47 components, of which 22 are radical species.

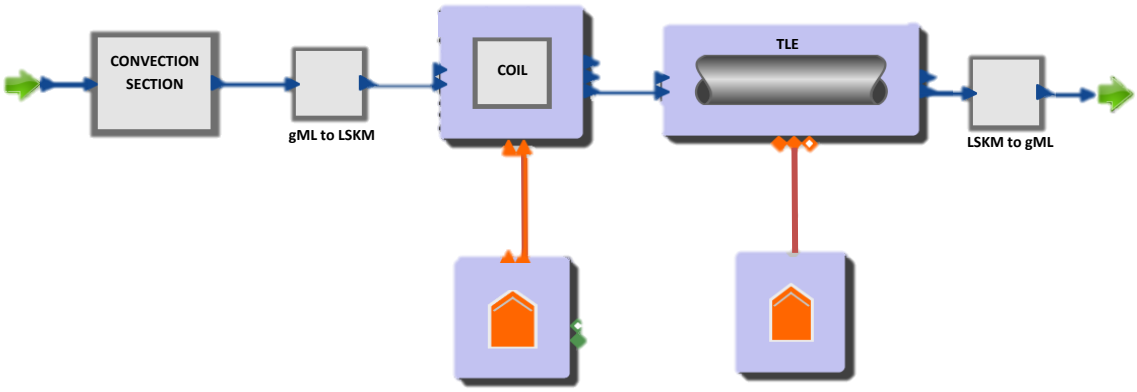

Figure 2- Furnace model from within gPROMS ProcessBuilder

3.1 Cracking tube model

In the cracking tube model, it is assumed a one-dimensional plug flow due to the turbulent flow, as well as low viscosity for the reaction side stream. This model calls for other sub-models: cracking kinetic model, coking kinetic model, fluid properties model, heat transfer coefficient model and friction factor coefficient model.

The cracking kinetic model is used to determine the reaction rate. For the case when the reaction is considered irreversible the equation 5 is used, while the equation 6 applies for the reversible reactions.

$$r_j = k_{fj} \prod_{k=1}^{NC} {C_i}^{n_{f,kj}} \quad (5)$$

$$r_j = k_{fj} \prod_{k=1}^{NC} {C_i}^{n_{f,kj}} - k_{rj} \prod_{k=1}^{NC} {C_k}^{n_{r,kj}} \quad (6)$$

In these equations k_{fi} and k_{ri} are the kinetic constants for the forward and reverse reactions respectively, $n_{f,ij}$ and $n_{r,ij}$ are the reaction orders and C_i is the concentration of component i. The kinetic constants for the forward reactions ($k_{f,j}$) are calculated according to the equation 7.

$$k_{f,j} = A_j T^{b_j} \exp\left(\frac{-E_{a,j}}{R.T}\right) \quad (7)$$

Where T is the fluid's temperature (K), A_j is the pre-exponential factor, $E_{a,j}$ is the activation energy of reaction j and b_j is the temperature exponent used to correct deviations from the Arrhenius equation. The kinetic constant for the reverse reaction is determined using the equilibrium constant. The equilibrium constant is calculated from the change of standard entropy (ΔS_j^0) and enthalpy (ΔH_j^0) during the reaction at system's temperature (T) and pressure (P)

The coking model was also developed during the present work. For this model it was considered that coke is formed through the dehydrogenation of Tar. Tar droplets form at high temperature in the pyrolysis furnace and are transported through the heat exchanger to the quench tower. When these droplets impinge on the wall surface they suffer dehydrogenation, originating coke [8]. Thus the coking reaction rate is considered to be the reaction rate of tar dehydrogenation.

In the coking model, the mass balance for Tar is done considering that the concentration of Tar is given by the difference between the Tar that is formed and is consumed by dehydrogenation.

The reaction rate of Tar formation (equation 8) is a function of acetylene and chloride concentrations, since it was concluded that the influence of other coking promoters were negligible.

$$r_{tar\ formation}(z) = k_{tar\ formation} C_{C_2H_2}(z) C_{Cl}(z) \quad (8)$$

$$r_{tar\ dehydrogenation}(z) = k_{tar\ dehydrogenation} C_{TAR}(z) \quad (9)$$

Both kinetic constants for Tar formation (equation 8) and Tar dehydrogenation (equation 9) follow the Arrhenius equation. The values for the activation energies and pre-exponential factors were obtained from a previous project done by PSE (EDCM1).

The fluid properties Model is used to determine all the properties required for the cracking tube model. Multiflash does not support radical species and their properties. For this reason, two sub models are called whether it is using a molecular based mechanism or a radical one.

When using the molecular properties model, the Multiflash FO is used to get the information regarding the

following properties of the mixture: Density, viscosity, thermal Conductivity, heat capacity, enthalpy and components molecular weight.

In the case of a radical based mechanism, the required properties are imported using the ReadData foreign object. From this file, the model receives the following properties for each component: molecular weight (M_w), enthalpy of formation (ΔH_f), entropy of formation (ΔS_f) and the parameters for heat capacity calculation (a_0, a_1, a_2 and b).

The enthalpy of the mixture is calculated based on the components enthalpy of formation, according to equation 10.

$$\Delta H = \sum_{i=1}^{NC} \left[\Delta H_{f,i} \times w_i\right] + \overline{C_p}\left[T(z) - T_{ref}\right] \quad (10)$$

Where T_{ref} is the reference temperature (298.15 K) and $\overline{C_p}$ is the average heat capacity of the mixture, given by the weighted average of the heat capacities of each component (equation 11).

$$\overline{C_p} = \sum_{i=1}^{NC} \frac{C_{p,i} \times w_i}{M_{w,i}} \quad (11)$$

The heat capacity of each component is determined using a 3rd order polynomial fitting as shown in equation 12.

$$C_{p,i} = \int_{T_{ref}}^{T} a_0.T^3 + a_1.T^2 + a_2.T + b.dT \quad (12)$$

Due to the lack of data, and considering the small concentration of radicals and by–products, the remaining properties (viscosity and thermal conductivity) were obtained using Multiflash for the main components (EDC, VCM and HCl).

3.1 Temperature Profile interpolation model

The temperature profile along the coil has an extreme importance in the accuracy of the results. In previous works, the temperature in the process was determined by the heat balanced based on the flowrates of the flue gas, fuel and air fed to the furnace. [9].

In this work, a model was developed where the temperature profile is determined by polynomial approximation, according to equation 13. This is achieved by considering as inputs to the model five real temperature measurements (T1 to T5 in Figure 3**Erro! A origem da referência não foi encontrada.**) as well as the respective axial positions. Besides this, the model also receives the Coil Inlet Temperature (CIT) from the upstream process simulation that corresponds to axial position zero.

$$T(z) = a + b.z + c.z^2 + d.z^3 + e.z^4 + f.z^5 + g.z^6 \quad (13)$$

Considering only the last two temperature measurements (T4 and T5 in Figure 3**Erro! A origem da referência não foi encontrada.**), a linear regre-ssion is applied in order to predict the temperature for axial position equal to 1 (T6 in Figure 3). By having the sixth temperature, the model is able to calculate the remaining constants of the equation 13 and determine the temperature profile inside the coil. Figure 3 shows the temperature profile in the coil, where the CIT appears in green, the five temperature measurements in blue and in purple is the sixth temperature determined by the linear regression.

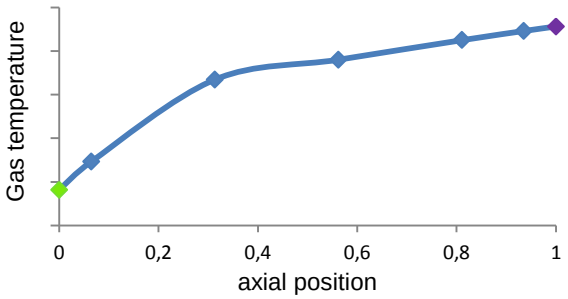

Figure 3 - Temperature Profile in the coil representation

4. Simulation Results

Following the EDC cracker set-up, it was necessary to test the performance and accuracy of the model (EDCM2), which has a considerable size.

In a previous work, an EDC cracker model was developed by PSE to simulate a specific industrial unit (EDCM1). Since it was considered that the model accurately described the system, at an early stage, EDCM1 was used to validate the results from the EDC cracker model developed in the present work (EDCM2).

To make this comparison possible, the required input variables were exactly the same in both models: feed composition and flow rate, coil inlet pressure (CIP) and Process gas temperatures (Temperature Profile Interpolation Model).

It was considered that the furnace feed was mainly EDC (>99 wt%) and a small amount of CCl_4. Carbon tetrachloride is known to be an efficient source of Cl radical and it can be used to promote the pyrolysis reaction. However, the Cl radical also acts as a promoter for undesirable coke formation. [1].

Regarding the output, this analysis was done focusing on the variables considered relevant to describe the good behaviour of the model: Conversion of EDC, outlet composition and pressure drop. The results for EDC conversion and outlet composition will reflect the accuracy of the cracking kinetic model. Regarding the outlet composition, besides acetylene, only the two main components were considered (EDC and VCM) since they alone make 80% of the total. Acetylene was only considered in this analysis due to its relevance for the coking model.

The pressure is mainly affected by coking deposition, thus it can be used as an indication of the efficiency of the coking kinetic model implemented in this work.

Along with the input variables already pointed out, the cracking and coking kinetics are also inputs given to the model.

As mentioned before, in the present work (EDCM2) the cracking kinetics from Choi et al. [1] were implemented. However, in the EDCM1 the kinetics used were the same but tuned according to the real data from the plant. On the other hand, the coking kinetics were strictly the same in both models. The activation energy and the pre-exponential factor were obtained from a previous work using the data from the real plant.

In Table 1, the deviation between the results of the two models is presented.

Table 1 – Deviation between the predictions from EDCM2 and EDCM1 (using purely Choi kinetics and Choi kinetics tuned to the real data)

Output variable		EDCM1 w/ Choi kinetics (%)	EDCM1 w/ Choi kinetics tuned to real data (%)
Pressure drop		0.11	1.4
Outlet flowrate	EDC	0.16	1.9
	VCM	0.11	1.4
	Acetylene	0.10	48

The objective is that the results from EDCM2 meet the results from EDCM1 with the tuned kinetics since this is the case that more accurately represents the reality. If in the EDCM1, the kinetics used were purely the ones from Choi all these errors would be within 0,2%, as shown in Table 1. Thus the deviations from EDCM1 with tuned kinetics and EDCM2 result from the difference between the cracking kinetics.

EDCM2 under predicts the acetylene composition in about 50%, as shown in Table 1. As acetylene is relevant for the coking formation, this discrepancy will have an impact on the pressure drop predictions.

It was then verified that the reaction rate for Tar formation from acetylene in EDCM2 was in average 3.5 times lower than the one predicted by EDCM1. Having this in consideration, the value of 3.5 was used as a factor to be multiplied by the kinetic constant of Tar formation from acetylene.

4.1 Simulation of a cycle (DynamicSimulation)

After evaluating the start of run simulation results, simulation of a complete cycle is performed, considering a period of around 12 months. The model inputs for the simulation were obtained from plant data and the cracking kinetics from Choi et al. were used.

The input variables analysed are the same as the ones mentioned before. While for the output variables, in this validation the outlet flowrates of the main components were considered instead of the outlet composition.

Considering the significant discrepancy in the acetylene concentration previously presented, for the coking kinetics two cases were considered (case A and B), presented in Table 2. Case A considers the coking kinetics previously described and already used for EDCM1 and EDCM2. In case B, the scaling factor influence is tested so the coking kinetics are the same as in case A but having the kinetic constant for tar formation from acetylene multiplied by 3.5. The model predictions for cases A and B were then compared to the available measurements, as it can be seen in Figures 4 to 8. For the first 20% of the cycle, real data was not reliable.

Table 2 – Description of the two cases considered in this analysis.

	Case A	Case B
Cracking kinetics	Choi et al. (2001)	Choi et al. (2001)
Coking kinetics	Parameters used in EDCM1	Same as Case A, but: $k_{Tar\ from\ acetylene} = 3.5 \times k_{Tar\ from\ acetylene}(\mathrm{EDCM1})$

Figure 4 shows the pressure drop predictions for both cases as well as the real data. In case B due to the scaling factor considered, the coke formation is bigger than in case A and the pressure drop in the coil increases. For this reason, the results from case B are better matched to the data, presenting an average deviation of 1,8% against 9,1% from case A.

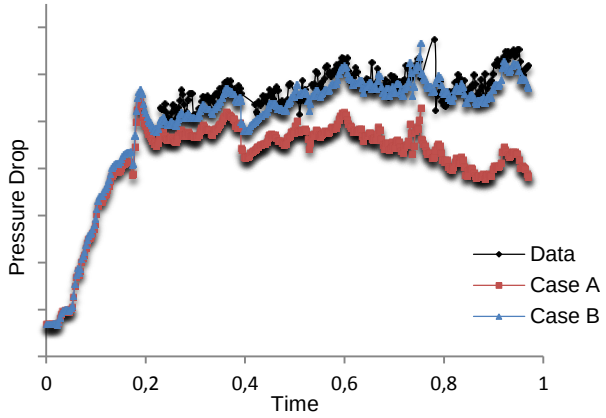

Figure 4 – Coil pressure drop predictions for case A and case B against real Data with time being normalised.

The effect of scaling factor on outlet flow rate predictions are not significant (<0.1%) as presented in the figures below (Figures 5 to 7). The average deviation between model predictions and real data is shown in Table 3.

Figure 5 shows the model predictions for EDC outlet flow rate from both cases and the respective data. The predictions have an average deviation of 4.4% and 4.5%, for case A and B, respectively.

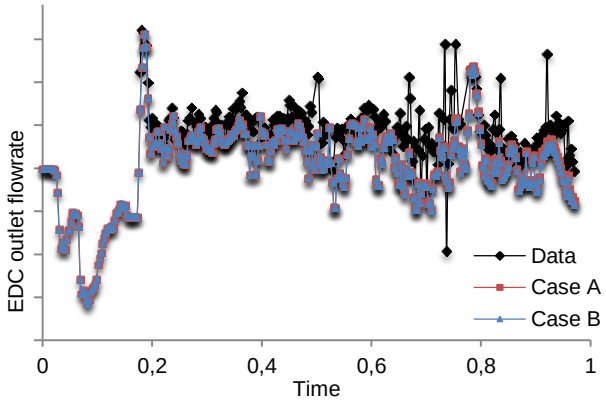

Figure 5 – EDC outlet flowrate predictions for case A and case B against real Data with time being normalised.

It is verified that the flowrate predicted by the model is in general lower than the real data, thus it seems that the model slightly over predicts EDC conversion. EDC conversion was calculated according to the equation 14, for cases A and B, as well as for the data. The EDC inlet was obtained from the unit real data which was used as an input to the model. The EDC outlet corresponds to the model predictions in each case.

$$\text{Conversion}_{\text{EDC}} = \frac{\text{EDC}_{\text{inlet}} - \text{EDC}_{\text{outlet}}}{\text{EDC}_{\text{inlet}}} \quad (14)$$

Figure 6 shows EDC conversion over time. For both cases, the EDC conversion is higher than the one calculated from the data in about 3.3%.

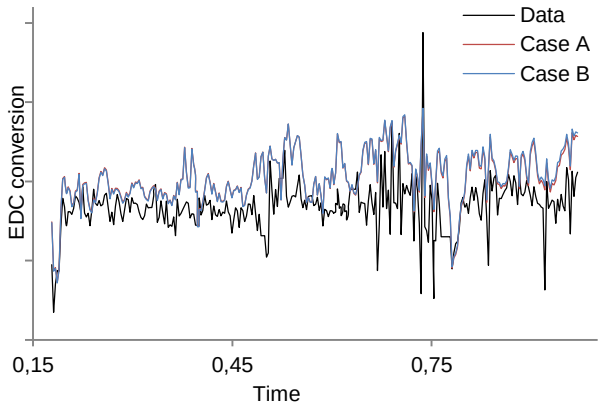

Figure 6 – EDC conversion in the outlet of the coil over time for case A and B and real data with time being normalised.

In figure 7 the results for VCM outlet flowrate are presented.

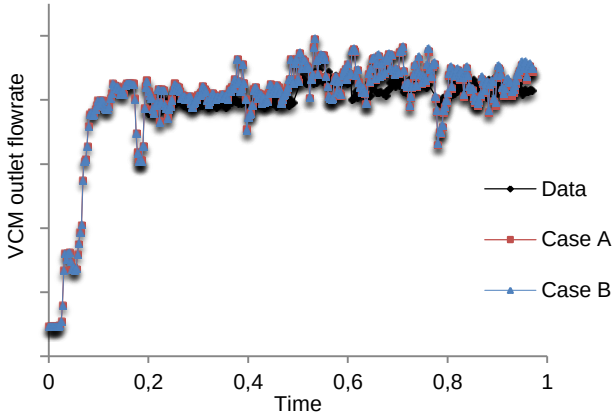

Figure 7 – VCM outlet flowrate predictions for case A and case B against real Data with time being normalised.

The model predictions have an average deviation from the real data of 1.8% for both cases. The model predicts in average a higher VCM outlet flowrate as it would be expected, since the model over predicts the EDC conversion.

Table 3 presents the average deviation from the model predictions and the real data for each output variable for both cases.

Table 3 – Average deviation from real data for each output variable predictions in case A and B.

	Case A (%)	**Case B (%)**
Pressure drop	9,1	1,8
EDC outlet flowrate	4,4	4,5
VCM outlet flowrate	1,8	1,8

5. State Estimation

In state estimation the objective is to adjust the model predictions to the real data, by changing some chosen related parameters.

To apply this technique, it is necessary to set variances for each adjusted parameter and the data corresponding to the output variables.

The variance in the case of the parameters can be seen as a measure of how much the model can vary its initial value, in order to meet the objective. A higher variance will allow larger change to the parameter value in comparison to a smaller variance. On the other hand, the variance of the real data can be seen as a measure of the confidence the model can have on it. A smaller variance indicates more accuracy of the measurement and state estimation would give more importance to such measurements in comparison to those with higher variance.

Table 4, shows the parameter to be adjusted by the model, “coking reaction rate adjustment” (CRR_{adj}) with the only objective of fit the pressure drop data.

The adjusted parameter is being multiplied by the expression used to calculate the coking reaction rate, as indicated by its name (eq.15)

$$r_{coke\ formation} = r_{tar\ dehydrogenation} \times CRR_{adj} \qquad (15)$$

For CRR_{adj}, an initial value of 1 is set, so if state estimation is not being employed, this value does not change, hence it will not affect any result. During state estimation, the model is allowed to change this parameter over time. If this parameter increases, the coking formation will also increase, leading to an increase in pressure drop. The decrease of this parameter will have the opposite effect.

Two cases were considered to be presented in this analysis (case 1 and 2), that vary from one another only in the variance defined to the coking reaction rate adjustment (table 4).

Following the line of thought described above, in case 1 the model is allowed to make more significant changes in the coking reaction rate adjustment parameter, since the variance set to this parameter is higher.

Table 4 – Parameters adjusted in state estimation as well as the output variables considered and respective variances for cases 1 and 2.

Type	Parameter/Variable	Variance	
		Case 1	Case 2
Adjusted Parameter	CRR_{adj}	5×10^{-6}	5×10^{-7}
Outputs Variable	Pressure drop	5×10^{-6}	5×10^{-6}
	EDC outlet flow rate	1×10^{20}	1×10^{20}
	VCM outlet flow rate	1×10^{20}	1×10^{20}

The variances set to the outlet flow rates are much higher than the order of magnitude of these variables (more than 1×10^{17} times). These values were defined to assure the variances are high enough for the model not to consider its data as relevant since it is only intended to meet the pressure drop data.

On the other hand, the variance set to pressure drop is relatively small. Hence the model will adjust the parameter with the only objective of meeting the pressure drop data.

Figures 9 to 12 show the model predictions with state estimation for both cases. The model predictions without state estimation (Simulation) are also presented, so it is possible to verify if state estimation has improved, or not, the results when compared to the real data.

Similarly to section 4, the data corresponding to the first 20% of the cycle was considered to be unreliable. In addition to that, for state estimation purposes, only the first 70% of the cycle was considered.

Figure 9 shows the state estimation results for pressure drop. The model predictions are similar for cases 1 and 2, with average deviations from real data of about 2.6% and 2.8%, respectively, as shown in table 5. Both cases show improvements when compared with the results without state estimation, which presents an average deviation of 4.1% (table 5).

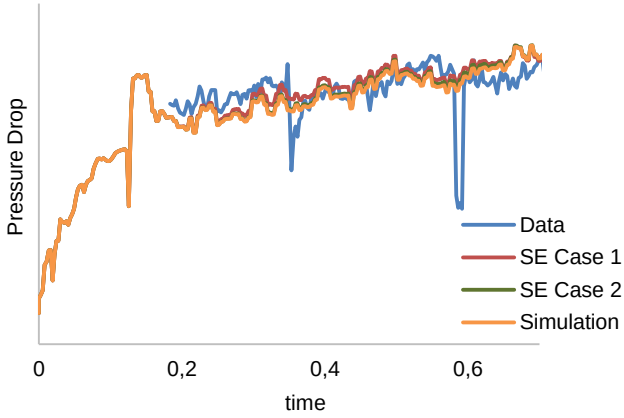

Figure 8 – Pressure drop predictions from state estimation against real data with time being normalised.

Despite the proximity of the results from case 1 and 2, the first one is still able to present better predictions. This is in agreement with what was expected, since in case 1 the model has more freedom to change the coking rate parameter in order to adjust the pressure drop predictions to the data.

Figure 10 shows the evolution of the reaction rate adjustment parameter over time. In the Simulation there is no change of this parameter from its initial value, since the model is not doing any state estimation.

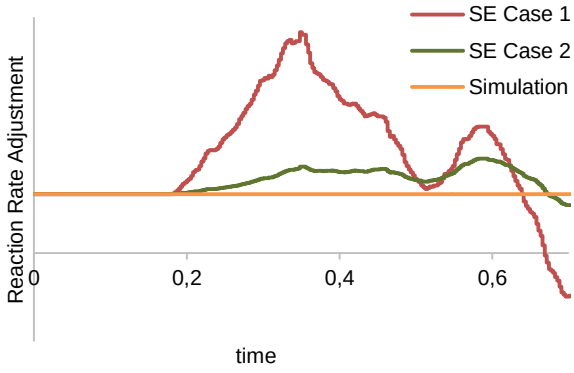

Figure 9 – Reaction rate adjustment variation from state estimation with time being normalised.

For the other two cases, it can be seen that the parameter does not vary at the beginning of the cycle. This is because in that period there is no data for pressure drop. Considering the model is only working towards the pressure drop adjustment if there isn't any data the model does not change the parameter.

As it was expected, in case 1 the coking reaction rate adjustment parameter will have more significant oscillations, since the set variance is higher than in case 2.

As the pressure drop increases, the model intensifies the coke formation, by increasing the coking reaction rate adjustment parameter. At some point, around 35% of the period, the data shows a lower peak

in pressure drop. Thus the model responds similarly by decreasing the parameter. Around 50% of the time, the parameter starts to increase again until another decrease in pressure drop occurs (around 58% of the time). The parameter continues decreasing since then, even assuming negative values at the end of the cycle.

The fact the parameter has a negative value means the coking reaction rate is also negative, which in reality would represent coke dissipation. Obviously in a real system, after being formed, coke will not disappear unless the operation is stopped and a decoking process is implemented.

In case 2, it can be verified the parameter has a similar behaviour than in case 1, but with oscillations of lower amplitude. Contrary to case 1, the parameter never reaches negative values.

Therefore, it is possible to verify that the variance settings on measurements and parameters are important to get meaningful values of the adjusted parameters.

For the remaining output variables, the results with state estimation (cases 1 and 2) show improvements when compared to the Simulation case.

In figure 11, the results for EDC outlet flow rate are presented. Case 1 and 2 have average deviations of 5.3% and 5.5%, respectively. Without state estimation, the model predictions present an average deviation of 6.3%.

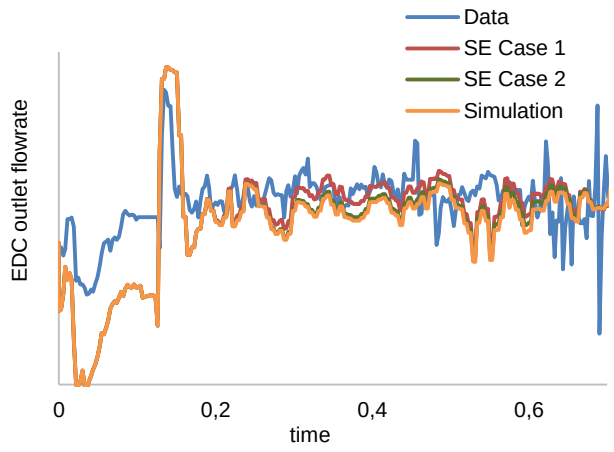

Figure 10 – EDC outlet flowrate predictions from state estimation against real data with time being normalised.

Figure 12 shows the results for VCM outlet flow rate. For this component, the model predictions present an average deviation of 3.4% for case 1 and 3.1% for case 2. The predictions without state estimation have an average deviation of 4.2%, which is, as expected, higher than the other two cases.

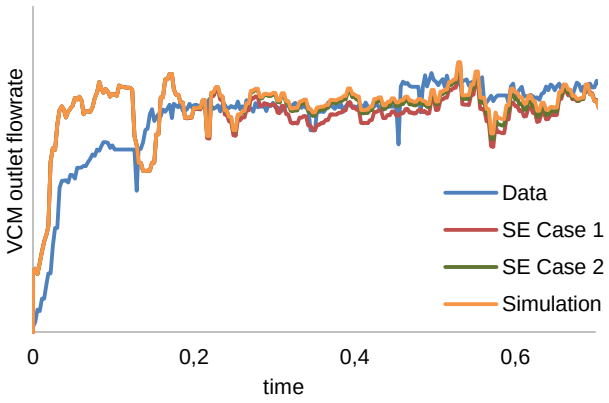

Figure 11 - VCM outlet flowrate predictions from state estimation against real data with time being normalised.

Table 6 shows the average deviations of the model predictions from real data, for each case considered and output variable.

Table 5 - Average deviations (%) of state estimation predictions from the real data for each case and variable

	Case 1	**Case 2**	**Prediction Only**
Pressure drop	2,58	2,76	4,54
EDC outlet flowrate	5,28	5,54	6.29
VCM outlet flowrate	3,38	3,12	3,56

Table 6 - Improvement of the model predictions with state estimation relatively to the prediction only case.

	Case 1	**Case 2**
Pressure drop	43,27	39,2
EDC outlet flowrate	16,1	12,0
VCM outlet flowrate	5,09	12,33

6. Kinetic Reduction

As a final step in this work, a study regarding the possibility of reducing the cracking kinetic scheme was attempted. The objective was to verify if all the 108 reactions included in the mechanism are in fact essential for the proper modelling of the furnace.

In this study, effect of each reaction (except the main reactions) on key output variables are analysed by disabling those reactions from the scheme.

The key output variables considered in this study are: EDC conversion and selectivity and outlet composition (considering the whole set of components)

Allowing a deviation of 0.1% from the model results when considering all the reactions, it would be possible to exclude 48 reactions. It is important to point out that these reactions are the ones that when excluded didn't affect the results more than 0.1% for any of the 54 variables considered. This was verified, even when all 48 reactions were excluded simultaneously.

In the furnace feed stream, there were only ethylene dichloride and carbon tetrachloride present. Hence it is not possible to conclude if these reactions would not be relevant in case there were more impurities in feed. It would be necessary to test that possibility, by including in the feed other components that may be present as impurities.

7. Discussion and Conclusion

In this work, an EDC cracker model (EDCM2) was setup using the furnace model libraries within gPROMS ProcessBuilder, to model the VCM production through EDC cracking.

In a previous work, an EDC cracker model (EDCM1) was developed by PSE to model a specific industrial unit. Since it was considered that EDCM1 is able to accurately simulate the reality of that unit, in an early stage, was used to validate the results from EDCM2. The same inputs were given to both models, excepting for the cracking kinetics. This difference lead to deviations between the results from the two models (table 2).

It was verified that EDCM2 under predicts acetylene outlet composition in about 50% when compared to EDCM1. Considering the relevance of this component as the main coke precursor, such deviation will have an impact on the pressure drop prediction, predominately affected by coke deposition. It was then verified that the coking reaction rate in EDCM2 was 3.5 times lower than EDCM1. Thus the value of 3.5 was used as a factor to be multiplied to the kinetic constant of Tar formation from acetylene.

Following this analysis, the model predictions from (EDCM2) was compared against data from a real plant such as pressure drop and the outlet flow rate of the main components (EDC and VCM).

Two cases were considered (cases A and B), similar to each other in all the aspects, except for the coking kinetics. In case B the reaction rate of coking formation is 3.5 times higher than in case A, by considering the scaling factor above mentioned. A sensitivity analysis was also performed considering higher and lower values for this scaling-factor, though it was concluded that 3.5 was actually the one presenting the best fit to the data.

The increment of coke formation in case B leads to an increase in pressure drop prediction with time. Thus the results from case B, with an average deviation of 1.8%, fit better the data than case A where pressure drop does not increase as much, presenting a deviation of 9.1%.

When analysing the model predictions for the outlet flowrate of the main components, it can be verified that these are not significantly affected by the factor applied in case B. The average deviations between both cases predictions and the real data are similar for all the components.

State estimations were also performed, focusing on the adjustment of pressure drop predictions by changing the coking reaction rate adjustment parameter. The model predictions were then compared to the results without state estimation (Simulation).

For all the output variables analysed, the results with state estimation (cases 1 and 2) show improvements when compared to the Simulation case. Cases 1 and 2 differ from one another in the variance defined for the adjusted parameter.

Pressure drop presents average deviations of 2.6 and 2.8% with state estimation, while the normal simulation would give results with about 4% of deviation.

EDC outlet flow rate presents average deviations of 5.3% and 5.5% for case 1 and 2, respectively. Without state estimations, the deviation would be 6.3%.

For VCM outlet flow rate the deviations are less significant than the previous component. In the Simulation case the results have an average deviation of about 4%, which is improved by state estimation reaching deviations of less than 3.5%.

Overall, with state estimation, it is possible to improve the model predictions for all the output variables. The variable for which state estimation had a more significant impact is, as expected, pressure drop with an improvement of around 40%. For the outlet flowrates improvements between 5 and 20% were achieved (table 6).

Even though the Case 1 is the one presenting an higher improvement in the accuracy of pressure drop predictions, that is achieved by taking the reaction rate adjustment parameter to not realistic values. Therefore, it is concluded that the variance settings on measurements and parameters are important to get meaningful values of the adjusted parameters.

The final step of this work was to study the possibility of reducing the cracking kinetic scheme. Allowing a deviation of 0.1% from the results considering the original mechanism, it was verified that 48 reactions could be excluded without compromising the results.

In the feed stream, only ethylene dichloride and carbon tetrachloride were considered for simulation purposes. However, the furnace feed may contain other components formed as by-products in the upstream process, predominately during oxychlorination. Some key impurities formed during that step are 1,1,2-trichloroethane, trichloroethylene, 1,1 and 1,2-dichloroethylenes, ethyl chloride, chloromethanes (methyl chloride, methylene chloride, chloroform), as well as polychlorinated high-boiling components [3]. Hence it

was not possible to conclude if these reactions would not be relevant in case there were more impurities in feed.

7.1 Future Work

Despite the work done, several improvements may and should be made to the model developed. This would include further testing of state estimation for the full cycle using fine tuning the different variances for the measurements and adjusted parameters. Further fine tuning of the state estimator could be performed by using data from multiple cycles.

It is also necessary to continue the kinetic reduction study initialized. In order to conclude about its feasibility, more tests would have to be done, considering other possible impurities in the furnace feed, such as chloroform, methyl chloride, ethyl chloride and 1,1,2-trichloroethane.

State estimation with the reduced kinetic scheme is expected to improve the computational performance significantly.

8. References

[1] B.-S. Choi, J. S. Oh, S.-W. Lee, H. Kim and J. Yi, "Simulation of the Effects of CCl4 on the Ethylene Dichloride Pyrolysis Process," *Industrial & Engineering Chemistry Research,* 2001.

[2] "ChemicalSafetyFacts.org," [Online]. Available: https://www.chemicalsafetyfacts.org/polyvinyl-chloride-post/. [Accessed October 2017].

[3] A. C. D. a. C. S. Bildea, "Vinyl Chloride Monomer Process," in *Chemical Process Design: Computer-Aided Case Studies*, Weinheim, WILEY-VCH Verlag GmbH & Co. KGaA, 2008, pp. 200-228.

[4] C. Li, G. Hu, W. Zhong, H. Cheng, W. Du and F. Qian, "Comprehensive Simulation and Optimization of an Ethylene Dichloride Cracker Based on the Onde-Dimensional Lobo_Evans Method and Computational Fluid Dynamics," *Industrial & Engineering Chemistry Research,* 2013.

[5] A. G. Borsa, "Industrial Plant/Laboratory Investigation and Computer modeling of 1,2-Dichloroethane pyrolysis," 1999.

[6] R. P. Tewarson, "Sparse Matrices," in *Mathematics in Science and Engineering*, Academic, 1973.

[7] D. Simon, Optimal State Estimation, Wiley, 2006.

[8] R. Schirmeister, J. Kahsnitz and M. Trager, "Influence od EDC severity on the Marginal Costs of Binyl Chloride Production," Industrial & Engineering Chemistry Research, 2009.

[9] R. Wong, "Advanced modeling of vinyl chloride monomer production via thermal cracking of ethylene dichloride," 2014.